Analysis of spatial and temporal patterns of on-road NO$_2$ concentrations in Hong Kong

Ying Zhu[a], Ka Lok Chan[a,b], Yun Fat Lam[c,d], Martin Horbanski[e], Denis Pöhler[e], Johannes Boll[a], Ivo Lipkowitsch[a], Sheng Ye[a], and Mark Wenig[a]

[a]Meteorological Institute, Ludwig-Maximilians-Universität München, Munich, Germany
[b]Remote Sensing Technology Institute, German Aerospace Center (DLR), Oberpfaffenhofen, Germany
[c]School of Energy and Environment, City University of Hong Kong, Hong Kong
[d]Guy Carpenter Climate Change Centre, City University of Hong Kong, Hong Kong
[e]Institute of Environmental Physics, Ruprecht-Karls-Universität Heidelberg, Heidelberg, Germany

Correspondence: Ka Lok Chan (lok.chan@lmu.de)

Abstract. In this paper we present an investigation of the spatial and temporal variability of street level concentrations of NO$_2$ in Hong Kong as an example for a densely populated megacity with heavy traffic. For the study we use a combination of open path remote sensing and in-situ measurement techniques that allows us to separate temporal changes and spatial patterns and analyse them separately. Two measurement campaigns have been conducted, one in December 2010 and one in March 2017. Each campaign lasted for a week which allowed us to examine diurnal cycles, weekly patterns as well as spatially resolved long term changes. We combined a long-path Differential Optical Absorption Spectroscopy (DOAS) instrument with a cavity enhanced DOAS and applied several normalizations to the data sets in order to make the different measurement routes comparable. For the analysis of long term changes we used the entire unfiltered data set, for the comparison of spatial patterns we filtered out the accumulation of NO$_2$ when stopping at traffic lights for focusing on the changes of NO$_2$ spatial distribution instead of comparing traffic flow patterns, and for the generation of composite maps the diurnal cycle has been normalized by scaling the mobile data with coinciding citywide path-averaged measurement results.

An overall descending trend from 2010 to 2017 could be observed, consistent with the observations of the ozone monitoring instrument (OMI) and the Environment Protection Department (EPD) air quality monitoring network data. However, long term difference maps show pronounced spatial structures with some areas, e.g. around subway stations, revealing an increasing trend. We could also show, that the weekend effect, which for the most part of Hong Kong shows reduced NO$_2$ concentrations on Sundays and to a lesser degree on Saturdays, is reversed around shopping malls. Our study shows that the spatial differences have to be considered when discussing city-wide trends and can be used to put local point measurements into perspective. The resulting data set provides a better insight into on-road NO$_2$ characteristics in Hong Kong which helps to identify heavily polluted areas and represents a useful database for urban planning and the design of pollution control measures.

1   Introduction

Nitrogen dioxide (NO$_2$) is one of the major air pollutant and plays a key role in both tropospheric and stratospheric chemistry. It participates in the catalytic formation of tropospheric ozone (O$_3$) and also contributes to the formation of secondary aerosols (Jang and Kamens, 2001; Huang et al., 2014) and causes acid rain. High NO$_2$ concentration is known to be toxic to human.

5   Nitrogen oxides (NO$_x$), defined as the sum of nitric oxide (NO) and NO$_2$, is released into the atmosphere from both natural and anthropogenic sources. Major sources of NO$_x$ include fossil fuel combustion, biomass burning, lightning and oxidation of ammonia (Bond et al., 2001; Zhang et al., 2003). In Hong Kong, vehicle emissions are the main source of NO$_x$. Similar to many metropolitan areas, a decreasing trend of ambient and roadside NO$_x$ levels has been observed (Carslaw, 2005; Keuken et al., 2009; Tian et al., 2011) which is contributed from the effective vehicular emission control measures in the past. However,

10   the pollution levels measured at both ambient and roadside air quality monitoring stations are still occasionally exceeded the world health organization (WHO) guideline values of 40 μg/m^3 (annual) and 200 μg/m^3 (hourly) for NO$_2$, with more frequent exceedance of hourly NO$_2$ with high values observed at roadside stations. A rising trend of NO$_2$/NO$_x$ ratio with reduction of NO$_x$ is recorded at the roadside monitor stations in Hong Kong, which means the reduction rate of NO$_2$ is slower than NO in recent years (Tian et al., 2011). Vehicular NO$_2$ is either primarily emitted at the tail pipe or secondarily formed from

15   oxidation of NO emission involving ozone and volatile organic compounds (VOCs) in the ambient (Muilwijk et al., 2016; Chang et al., 2016). The increase of NO$_2$/NO$_x$ ratio could either relate to the upgrades of vehicle engines and catalytic filters or changes in the composition and ambient level of VOCs. However, NO$_2$ concentration changes rapidly with time and has a very strong spatio-temporal variability, which is often unknown in urban areas (Longley et al., 2015). Regular roadside air quality monitoring stations are not sufficient to capture these variations and could not provide an overview of the roadside

20   pollution situation representative for Hong Kong. Therefore, it is necessary to perform on-road mobile measurements for better understanding the pollutant distribution and spatial coverage of NO$_2$ for the entire city.

In order to capture the spatial and temporal variability of NO$_2$ concentrations in the central metropolitan area of Hong Kong, we use a combination of two different differential optical absorption spectroscopy (DOAS) techniques, a long path DOAS (LP-DOAS) and a cavity enhanced DOAS (CE-DOAS), as well as an ultraviolet (UV) based dual beam in-situ ozone monitor

25   (Model 205, 2B Technologies). CE-DOAS is a relatively new spectroscopic measurement technique which uses an optical resonator to produce a long light path to enhance the absorption signal within a limited space (Platt et al., 2009). Sensitive measurements of trace gas have already been demonstrated by Langridge et al. (2006); Venables et al. (2006); Washenfelder et al. (2008); Thalman and Volkamer (2010); Min et al. (2016); Chan et al. (2017b). Compared to other in-situ NO$_2$ monitoring techniques, CE-DOAS is insensitive to other reactive nitrogen (NO$_y$) in the atmosphere, making it a better option for small

30   spatial scale measurements and detection of spatial variation of trace gases. Its high accuracy allows fast sampling which is important for mobile measurements.

Mobile measurements are an effective tool to obtain the spatial and temporal variations of highly dynamic on-road pollutants. Therefore, it has been widely used for determining on-road vehicle emission factors (Vogt et al., 2003; Uhrner et al., 2007; Ning et al., 2012) and assessing the impacts of urban planning on air quality (Rakowska et al., 2014; Chan et al., 2017b).

Mobile CE-DOAS measurements of on-road NO_2 were performed in December 2010 and March 2017. The mobile measurements were used to investigate the relationship between on-road and ambient air quality. In addition, LP-DOAS measurements were performed to investigate the temporal variation of general ambient NO_2 in Hong Kong. Details of the mobile CE-DOAS and LP-DOAS experimental setups are presented in section 2. In section 3.2, the data filtering and normalization algorithms applied to the mobile measurement data are introduced. The mobile NO_2 measurements are then analysed together with LP-DOAS and local monitoring station data for the long term trends, and results are shown in section 3.3. Section 3.4 presents the analysis of the characteristics of the weekend effect for different parts of the city. In addition, the spatial patterns of on-road NO_2 and the identification of pollution hotspots are presented in section 3.5.

2   Methodology

2.1   Mobile cavity enhanced DOAS

A CE-DOAS instrument was employed for mobile measurements using a sampling inlet positioned on top of the front part of the vehicle at a height of about 1.5 m above ground. The measurements were performed in December 2010 and March 2017 and divided into two parts, (a) measurement along a standard route that covers large part of the urban area in Hong Kong and (b) single measurement in different areas that are not covered by the route. The regular route covers Mong Kok, Central and Causeway Bay which are the busiest areas in Hong Kong (see Figure 1). The standard route measurements were performed 2 to 3 times per day in order to cover non-rush hours, morning and evening rush hours. The varying route measurements were mostly performed during non-rush hours which aims to provide better spatial coverage and to identify pollution hotspots. Measurements performed in 2010 focus more on the on-road NO_2 spatial distribution and the identification of pollution hotspots. Therefore, the 2010 measurements include more non-standard route measurements to have a better spatial coverage. On the other hand, the objectives of the 2017 measurements were refined to investigate the spatio-temporal variations over major pollution hotspots, that are mostly concentrated in the city center. As a result, we focused more on the standard route measurements over the city center in 2017.

The principle of the CE-DOAS (Platt et al., 2009) is similar to that of the cavity enhanced absorption spectroscopy (CEAS) (Fiedler et al., 2003). The measured absorption spectrum of an incoherent broad band light source (e.g. LED) is used to determine the concentration of trace gases, which allows the application of the DOAS technique for the detection of multiple trace gases by a single instrument.

A schematic diagram of the CE-DOAS instrument is shown in Figure 2. The CE-DOAS consists of a blue LED light source, an optical resonator with two high reflective mirrors, a spectrometer and an air sampling system. Dielectric coated high reflective mirrors (reflectivity >99.98 % at 440 nm) are placed at both ends of the sampling cell to form an optical resonator. Light from the high power blue LED (CREE XR-E royal blue, 440 nm - 455 nm FWHM) is coupled into the optical resonator by a convex lens with a focal length of 25 mm. Light escaped from the other side of the optical resonator is coupled to an optical fiber with a numerical aperture of 0.22 by a convex lens with a focal length of 50 mm and an aluminum mirror. The transmitted light is redirected to the spectrometer for spectral analysis through the optical fiber. Spectra are recorded by an
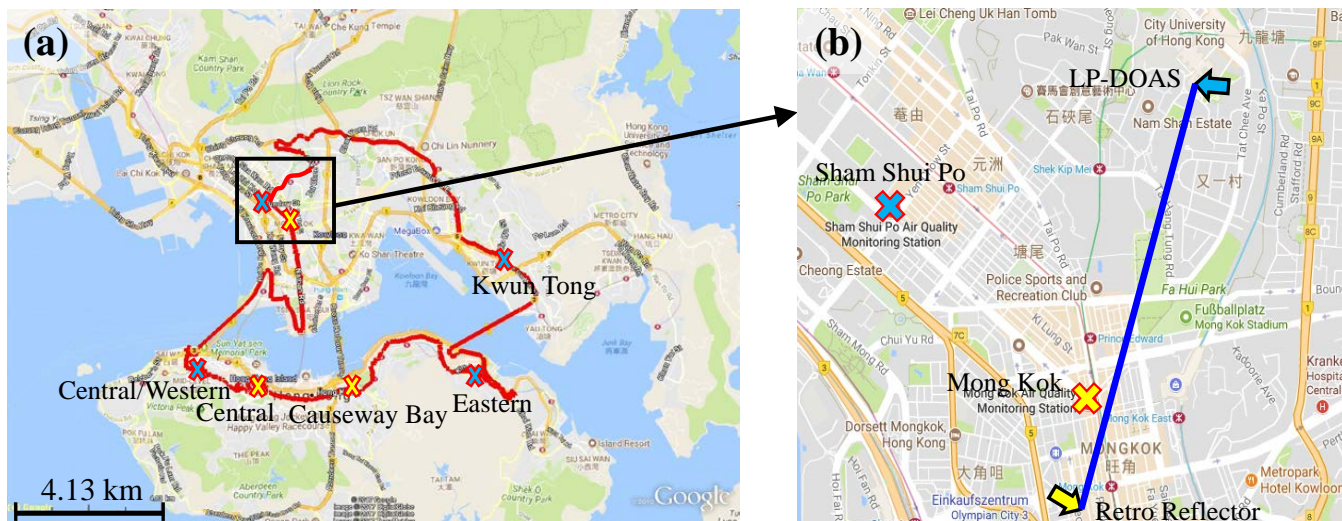
Figure 1. Map of Hong Kong city center. (a) The standard measurement route; (b) the location of LP-DOAS. Yellow crosses indicate 3 roadside EPD monitoring stations while blue crosses represent 4 ambient EPD monitoring stations. The blue line indicated in (b) represents the optical path of the LP-DOAS.

Avantes spectrometer (AvaSpec-ULSi2048L-USB2) with a Sony ILX511 charge coupled device (CCD) detector. The spectral range of the spectrometer is adjusted to 395 nm - 492 nm with a spectral resolution of 0.47 nm (FWHM). The sampling cell is made by a Teflon pipe with length of 50 cm and a sampling volume of 286.3 cm^3. The sample flow of the system is achieved by a direct current vacuum pump located at the outlet side of the sampling chamber. A Teflon filter is placed in front of the
5   inlet of the sampling cavity to avoid aerosols entering the sampling cavity and affecting the optical path by scattering and contamination of the high reflective mirrors. The time resolution of the CE-DOAS was adjusted to 4 seconds during the mobile measurement. The detection limit of the instrument is 1 ppbv. More detailed description of the CE-DOAS instrument can be found in Platt et al. (2009); Chan et al. (2017b).

In this study, the software DOASIS (Kraus, 2005) was used for the CE-DOAS spectral evaluation. The CE-DOAS spectral
10 fit is performed in the wavelengths from 435.6 nm to 455.1 nm, which includes several strong NO$_2$ and water vapor absorption bands. Reference absorption cross sections of NO$_2$ (Vandaele et al., 2002), H$_2$O (Rothman et al., 2003), Glyoxal (CHOCHO) (Volkamer et al., 2005) and O$_4$ (Hermans et al., 1999) were included in the DOAS fitting.

2.2   Long path DOAS observations

A Light Emitting Diode (LED) based LP-DOAS system was installed on the roof top of the City University of Hong Kong
15 building, providing measurement of near surface NO$_2$. The retro reflectors were placed on a high rise building located at the center of Kowloon, realizing an optical path of 1.9 km (total absorption path of 3.8 km). The spectral range of the spectrometer was adjusted from 400 nm to 462 nm with a spectral resolution of 0.4 nm (FWHM). The average altitude of the LP-DOAS
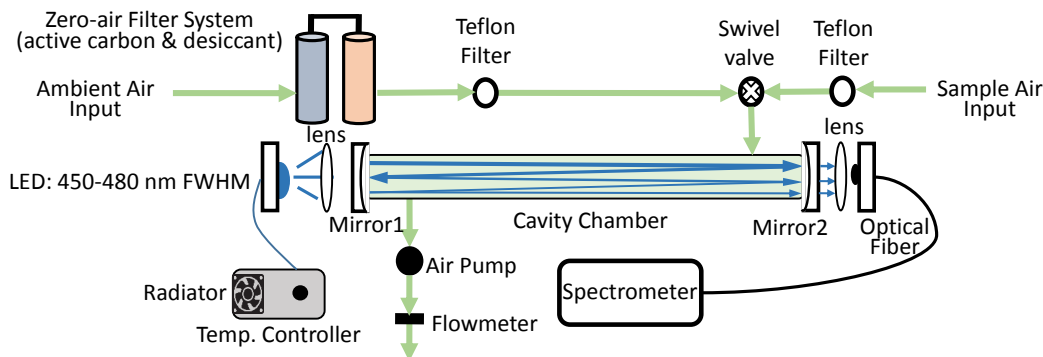
Figure 2. Schematic diagram of the experimental setup of the CE-DOAS.

light path is ∼50 m above ground level covering a long light path over the urban area of Hong Kong, providing better over of the spatial distribution of ambient NO_2 level. Details of the experimental setup and the data retrieval procedure of the LP-DOAS can be found in Chan et al. (2012, 2017a). When focusing on the spatial variations, we used ambient NO_2 values measured by the LP-DOAS to normalize for the temporal dependency of the mobile CE-DOAS measurements. Since the

5 mobile measurements record data from different parts of the city at different times of the day, the diurnal variability has to be normalized in order to produce a concentration map that is representable for daily average concentration of NO_2. Details of the normalization procedure are presented in section 3.2.

2.3 Local air quality monitoring network

Ambient NO_2 data in Hong Kong were acquired from the air quality monitoring network of Hong Kong which is operated by

10 the Environmental Protection Department (EPD). The air quality monitoring network comprises 13 ambient and 3 roadside monitor stations (see Figure 1 for the locations of some of the stations). The ambient stations are located at different altitude and in general above 10 m a.g.l., while the road side stations are measuring at 3 m a.g.l.. The measurements cover both urban and rural areas in Hong Kong. The NO_2 and NO_x concentrations are measured by in-situ chemiluminescence NO_x analyzer. Ultra-violet (UV) absorption O_3 analyzer is used for O_3 monitoring. More details of the air quality monitoring network can

15 be found on http://www.aqhi.gov.hk/en/monitoring-network/air-quality-monitoring-network.html. Hourly NO_2 concentrations from seven nearby air quality monitoring stations were used to compare to LP-DOAS and CE-DOAS NO_2 measurements. In addition, NO_2, NO_x and O_3 data from the monitoring stations are used for long-term trend analysis.

2.4 OMI Satellite observations

The Ozone Monitoring Instrument (OMI) is a passive nadir-viewing satellite borne imaging spectrometer (Levelt et al., 2006)

20 on board the Earth Observing System's (EOS) Aura satellite. The instrument consists of two charge-coupled devices (CCDs) covering a wavelength range from 264 nm to 504 nm. A scan provides measurements at 60 positions across the orbital track
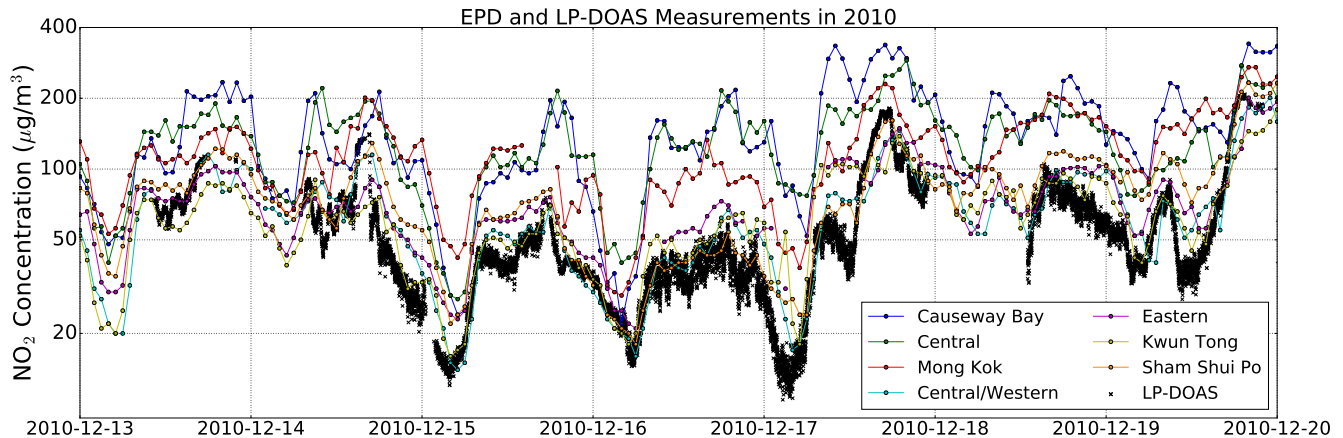
Figure 3. Time series of NO$_2$ concentration measured by LP-DOAS and EPD Monitoring stations during the measurement campaign in 2010.

covering a swath of approximately 2600 km. The spatial resolution of OMI varies from $\sim$320 km^2 (at nadir) to $\sim$6400 km^2 (at both edges of the swath). The instrument scans along 14.5 sun-synchronous polar orbits per day, providing daily global coverage observations.

In this study, NASA's OMI NO$_2$ standard product version 3 (SPv3) is used (Krotkov et al., 2017). The slant column densities (SCDs) of NO$_2$ are derived from Earth's reflected spectra in the visible range (402 - 465 nm) using an iterative sequential algorithm (Marchenko et al., 2015). The OMI NO$_2$ SCDs are converted to vertical column densities (VCDs) by using the concept of air mass factor (AMF) (Solomon et al., 1987). The AMFs are calculated based on NO$_2$ and temperature profiles derived from the Global Modeling Initiative (GMI) chemistry transport model simulations with a horizontal resolution of 1° (latitude) $\times$ 1.25° (longitude) (Rotman et al., 2001). Separation of stratospheric and tropospheric columns is achieved by the local analysis of the stratospheric field over unpolluted areas (Bucsela et al., 2013).

3 Results and Discussion

3.1 NO$_2$ measurement comparison

Our LP-DOAS measurements of atmospheric NO$_2$ in Hong Kong started in December 2010. The data shows significant diurnal, weekly and seasonal variability. The daytime annual average NO$_2$ concentration measured by the LP-DOAS from 2011 to 2015 is 47.5 μg/m^3. A decreasing trend can be observed (see section 3.3 for more detailed discussion), but they all still higher than the annual average of 40 μg/m^3 in WHO guideline (same standard as the Hong Kong air quality objective for NO$_2$). Additionally, episodes of high NO$_2$ levels are occasionally recorded, especially from long range transportation of air pollutants from mainland China (Kuhlmann et al., 2015).

A time series of NO_2 concentrations measured by LP-DOAS and EPD monitoring stations are shown in Figure 3. On one hand, both LP-DOAS and EPD measurements show similar variation pattern with higher values during daytime and lower values at night. On the other hand, LP-DOAS and different EPD stations measurements also demonstrate different characteristics of NO_2. The significant spatial dependency of NO_2 is also confirmed in long-term changes (see section 3.3 for

5   more detailed discussion). All measurements show an elevated NO_2 level during morning (8:00 to 10:00) and afternoon (17:00 to 19:00) rush hours. However, the absolute concentration measured by different stations varies in a wide range. In addition, differences in measurement height also contribute to differences among these measurements. In order to have a better overview of the NO_2 spatial distribution, temporal variation and their emission source pattern, we performed mobile measurements of on-road NO_2 using a CE-DOAS instrument. On road measurement can easily be influenced by the traffic condition, e.g.,

10   accumulation of emission during traffic congestion, and the diurnal variation of ambient NO_2. In order to correct for these effects in the mobile measurement, we have filtered data which is influenced by traffic condition and normalized the on-road measurement for diurnal variation of NO_2.

3.2   Data filtering and normalization

3.2.1   Comparison of concentrations during fluent traffic and traffic congestion

15   Traffic congestion can result in higher pollution levels due to accumulation of vehicle emissions, caused by less turbulent mixing with cleaner air and longer NO to NO_2 reaction time. It has been observed that high concentrations of NO_2 were recorded during low speed driving in our measurements, i.e. in a traffic jam or waiting in front of a traffic light. Figure 4 shows the time series of vehicle speed and measured NO_2 concentration during a traffic congestion on 2nd Mar 2017. Note that the vehicle speed is calculated from the GPS data with an error about 0.6 m. Converting the error into vehicle speed would be

20   1.4 km/h. Therefore, the vehicle speed is never zero even if the vehicle stops. In the example shown in Figure 4, the vehicle slowed down and stopped for half a minute at a traffic light. The NO_2 level goes up from about $100\,\mu g/m^3$ to more than $400\,\mu g/m^3$. The NO_2 level rises about 8 s after the vehicle stopped. When the vehicle started moving again, the measured NO_2 level gradually dropped back to the pre-stop level within 20 s.

In order to separate data that is influenced the NO_2 spikes induced by traffic congestion or idling, we filtered data from 8 s

25   after the vehicle speed drop below 5 km/h to 20 s after the vehicle speed goes above 5 km/h again. In order to avoid filtering data due to poor GPS signal, this filter only applies when the vehicle speed is below 5 km/h for more than 8 s. The lag time shown in this case is 8 s. It is the combination of accumulation of NO_2 in ambient and the lag time of the instrument. The lag time of the instrument is $\sim$4 s, while the time of accumulation of NO_2 varies with the ambient condition. The average NO_2 concentrations for standing condition are $239\,\mu g/m^3$ which is 14.5 % higher on average. We filter out traffic light or traffic jam stops only to

30   have a consistent NO_2 spatial distribution under fluent driving condition for the direct comparison of measurements in different days and years, in order to focus on the concentrations instead of the congestion patterns. This filter criterion removed 37 % and 30 % of the total number of measurement data in 2010 and 2017. However, since the filter mainly removes measurements
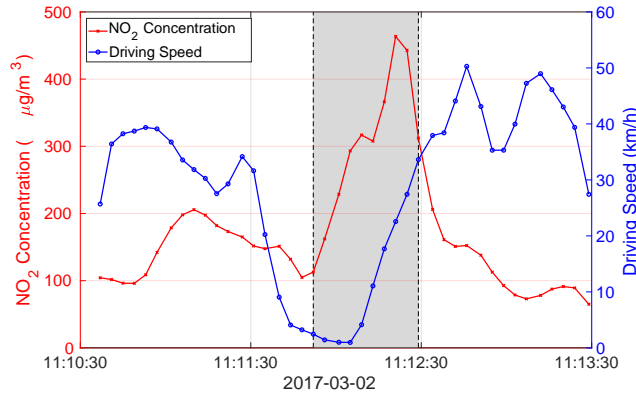
Figure 4. Time series of the driving speed and the coinciding NO_2 concentration during traffic congestion. Data in gray area will be filtered out in later analysis.

at low speed or standing, only 10 % and 11 % of the spatial points were removed for 2010 and 2017, respectively. This filter is only applied to generate maps for comparison.

3.2.2   Normalization of the diurnal cycle

In order to separate the NO_2 spatial and temporal variability and show a representative spatial distribution of NO_2 in Hong Kong, we developed an algorithm using LP-DOAS measurements to normalize for the diurnal variations. Although the LP-DOAS measurement covers a long light path over the urban area in Hong Kong, the NO_2 values provided might still not be representative for all measurement areas due to local influences. Therefore, we use a normalized long term average of diurnal NO_2 cycle for each weekday to correct for the temporal variation effect. The normalized data is less depending on outliers caused by the overpass pollution plume and can also interpolate data gaps due to instrumental problems and bad weather.

LP-DOAS measurements of atmospheric NO_2 for each day are first normalized by dividing by the daily mean NO_2 concentration. The resulting normalized NO_2 level are then averaged for each day of the week over a period of 2 years to obtain a representative diurnal NO_2 variation pattern. The normalized and averaged diurnal NO_2 variation pattern of the corresponding weekday is scaled and shifted to fit the normalized LP-DOAS measurement for each day during the mobile measurement campaign. The inverse of the 1 σ (standard deviation) variation of the 2-year averaged and normalized NO_2 level is used as weighting in the least squares regression to scale and shift the long term average diurnal pattern. In order to avoid single high value affecting the whole regression, normalized NO_2 level exceeded the 1 σ variation of the 2-year averaged and normalized NO_2 level were not considered in the regression process. Figure 5 shows the normalized NO_2 concentration measured by the LP-DOAS on 17th Dec 2010. Normalized 2-year Friday mean NO_2 diurnal pattern, the diurnal pattern of scaled NO_2 measurement taken on 17th Dec 2010 and normalized EPD monitoring data are shown as well. All data illustrate similar characteristics with significant peaks in the morning (8:00 to 10:00) and evening (17:00 to 19:00) rush hours. Compared to the original LP-
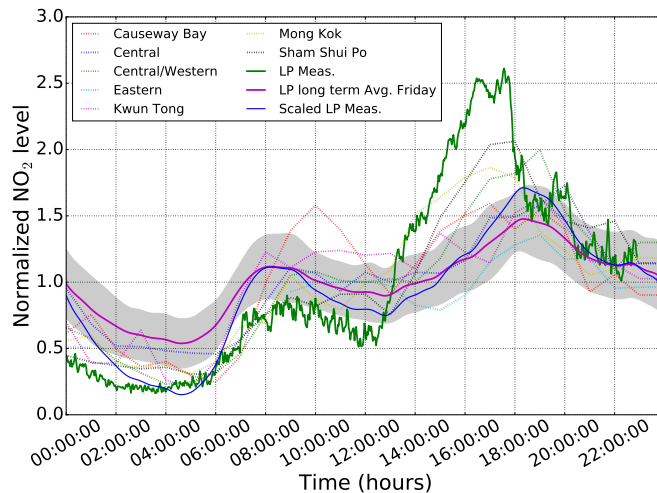
Figure 5. Normalized diurnal cycle of NO_2 on Friday in Hong Kong in 2010 measured by the LP-DOAS and EPD monitoring stations. EPD measurements on 17th Dec 2010 from 7 monitoring stations are indicated as dashed line. The green curve represents LP-DOAS measurement while purple line is the 2 years averaged diurnal pattern with shadowed area of the 1 σ standard deviation variation. The blue line shows the scaled and shifted diurnal pattern of ambient NO_2 on Friday, 17th Dec 2010.

DOAS measurements, the fitted mean diurnal NO_2 pattern matches better with measurements from most of the EPD monitor stations, indicating the fitted diurnal pattern better represent the general condition in Hong Kong. The fitted long term diurnal pattern is then used to correct for the diurnal effect of the mobile measurement. Mobile measurements are multiplied by the simultaneous NO_2 level of the resulting normalized LP-DOAS diurnal pattern to obtain a more representative value for the
5   measurement areas.

3.3   Long-term trends of NO_2

On road CE-DOAS measurements are analyzed together with LP-DOAS and EPD monitors data to investigate the long term trend of on-road and ambient NO_2. The observed trends at different locations are compared to the changes of the mobile on-road CE-DOAS NO_2 measurements in 2010 and 2017 taken within 100 m radius of the 3 EPD roadside stations or within
10   1 km radius of the center of the LP-DOAS measurement path (Figure 6a, b, c and d), in order to illustrate the differences between on-road mobile and road side stationary measurements and to examine the consistency of the long term trend of road side NO_2 derived from stationary measurements. The time series represent monthly averaged ambient NO_2 concentrations measured during daytime. OMI satellite observations of monthly average tropospheric NO_2 VCDs over Hong Kong are shown in Figure 6e. The data were filtered for cloud fraction larger than 50 % and averaged for OMI pixel within 50 km of the
15   measurement site. The on-road CE-DOAS NO_2 measurements are in general much higher than the ambient monitor stations data. This is mainly due the difference in measurement height. The inlet of our on-road mobile measurement platform was set
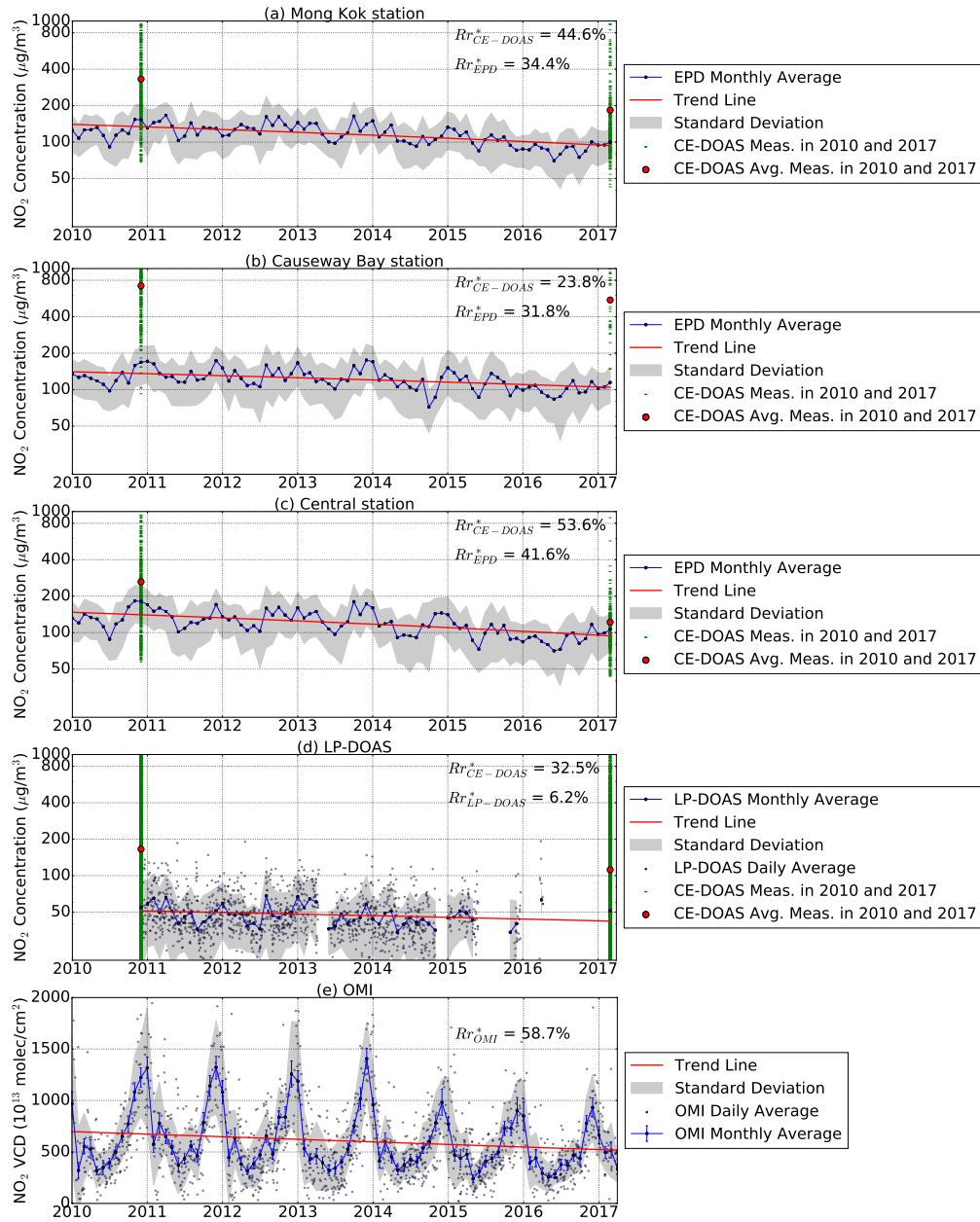
Figure 6. Monthly averaged daytime NO$_2$ concentration from Jan 2010 to Mar 2017 measured by three EPD stations and LP-DOAS. Red dots indicate the averaged NO$_2$ concentration measured by the CE-DOAS within 100 m radius of (a) Mong Kok, (b) Causeway Bay and (c) Central roadside station. (d) shows the CE-DOAS measurements within 1 km radius of the center of the LP-DOAS measurement path and monthly daytime averaged ambient NO$_2$ levels observed by the LP-DOAS. (e) shows the monthly averaged OMI tropospheric NO$_2$ VCDs over Hong Kong. The reduction rates Rr indicated on the figures are calculated by taking the relative difference between averaged data taken in December 2010 and March 2017. Low reduction of LP-DOAS is due to sparse measurements in March 2017.
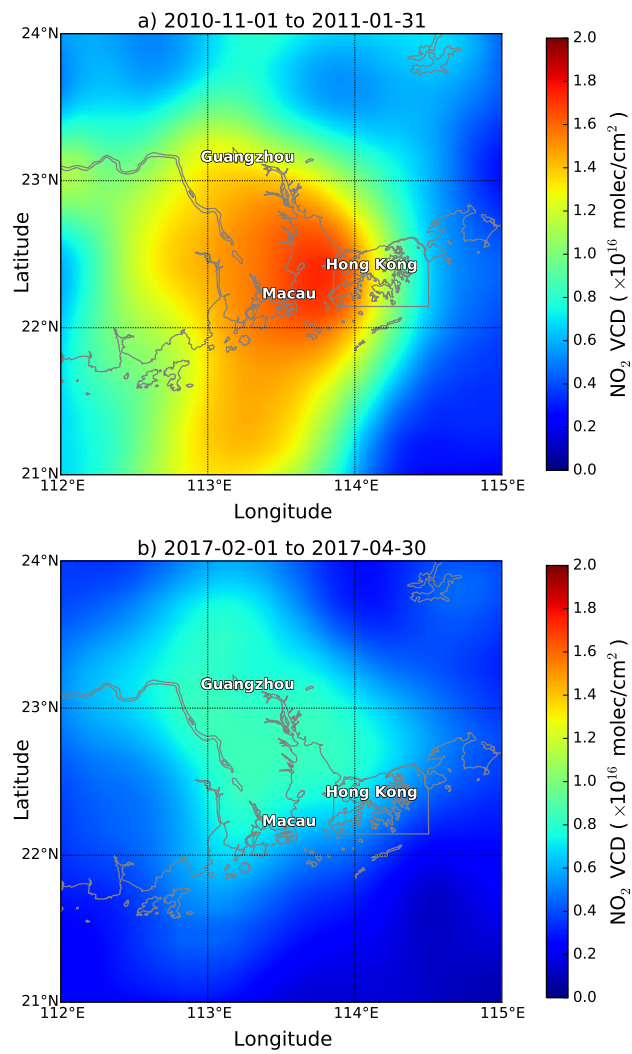
Figure 7. Averaged OMI tropospheric NO$_2$ VCDs over Pearl River Delta a) from 1st of Nov 2010 to 31st Jan 2011 and b) from 1st Feb 2017 to 31st Apr 2017.

up at 1.5 m a.g.l, while the EPD road side stations were measurement at 3 m a.g.l. and the ambient stations were located at even higher altitudes. As the tail pipes of vehicles are usually at 10 - 30 cm a.g.l., our mobile measurement inlet is much closer to the emission sources and therefore in general measures higher NO_2 concentrations.

On-road, ambient, and satellite measurements of NO_2 all show a decreasing trend. Ambient NO_2 levels measured by the LP-
5   DOAS show a descending trend with a rate of 2.5 % per year. Stronger decreasing trends of roadside NO_2 are observed by EPD in Mong Kok, Causeway Bay and Central roadside station with annual decreasing rates of 4.4 %, 3.3 % and 4.8 %, respectively. A similar reduction rate is also observed by on-road CE-DOAS measurements. Comparing the CE-DOAS measurement taken in 2010 and 2017, on-road NO_2 levels are overall reduced by 28 % for areas along the standard measurement route which would correspond to an annual decreasing rate of 4.0 %. NO_2 levels in 85 % of the measurement area are significant reduced (>1 ppbv)
10   by 37 % on average, whereas NO_2 levels in 14 % of the area are elevated (>1 ppbv) by 22 % on average. The reduction rate for on-road NO_2 levels around the EPD roadside monitor stations varies from 24 % to 54 %. This reduction change can also be observed from space by OMI satellite. Tropospheric NO_2 VCDs show a descending trend with a rate of 3.7 % per year. In addition, Figure 7a and b show tropospheric NO_2 VCDs over the Pearl River Delta from 1st of Nov 2010 to 31st Jan 2011 and from 1st Feb 2017 to 31st Apr 2017, respectively. In general, tropospheric NO_2 VCDs are reduced by ∼50 % (7 % per year)
15   over Hong Kong, while the reduction over Pearl River Delta is ranging from 30 - 60 %.

Averaged on-road NO_2 concentrations measured along the standard route during December 2010 and March 2017 are shown in Figure 8a and b, the differences in Figure 8c. The measurement routes are slightly different due to road constructions and maintenance. The two measurement campaigns were performed in winter and early spring. We have analyzed the meteorological parameters including temperature, humidity, wind speed and wind direction taken during the two measurement campaigns.
20   The results show that the meteorological conditions are quite similar during the two campaigns. In general, a significant reduction (ranging from 20 % to 50 %, and on average 4 % per year) of on-road NO_2 can be observed which is consistent with the LP-DOAS and EPD monitor data. The reduction of on-road NO_2 level along Nathan Road, the busiest road in Kowloon, is ranging from 50 % to 60 % (around 7 % to 8 % per year). On the other hand, an enhancement of NO_2 level can be observed around subway stations, e.g., Hong Kong University station, Kwun Tong station, Diamond Hill station, Ngau Tau Kok station,
25   etc. It probably reflects the fact that there are more bus terminals or bus stops surrounding metro stations in 2017 compared to 2010. Data from the transport department shows that the total number of licensed franchised bus has slightly increased by 3 % from 5729 in 2010 to 5916 in 2016 (http://www.td.gov.hk/en/transport_in_hong_kong/transport_figures/monthly_traffic_ and_transport_digest/index.html). Although the number of franchised bus only has a small contribution to the total number of vehicle in Hong Kong (608 thousands in 2010, 746 thousands in 2016), franchised buses can account for up to 40 % of
30   the traffic at busy traffic corridors (http://www.info.gov.hk/gia/general/201512/31/P201512310204.htm). Average daily public transport usage also increased from 11.6 millions time per day in 2010 to 12.6 millions time per day in 2016. According to the annual reports of Transport International Holdings Limited, the parent company of the Kowloon Motor Bus Company, the largest franchised bus operator in Hong Kong, the total number of buses running by the company increases slightly from 3988 in 2010 to 4162 in 2016. However, the number of bus routes reduced from 393 in 2010 to 384 in 2016. These changes are
35   mainly due to the reformation of the operational strategies of the franchised bus operators. Due to the expansion of the metro
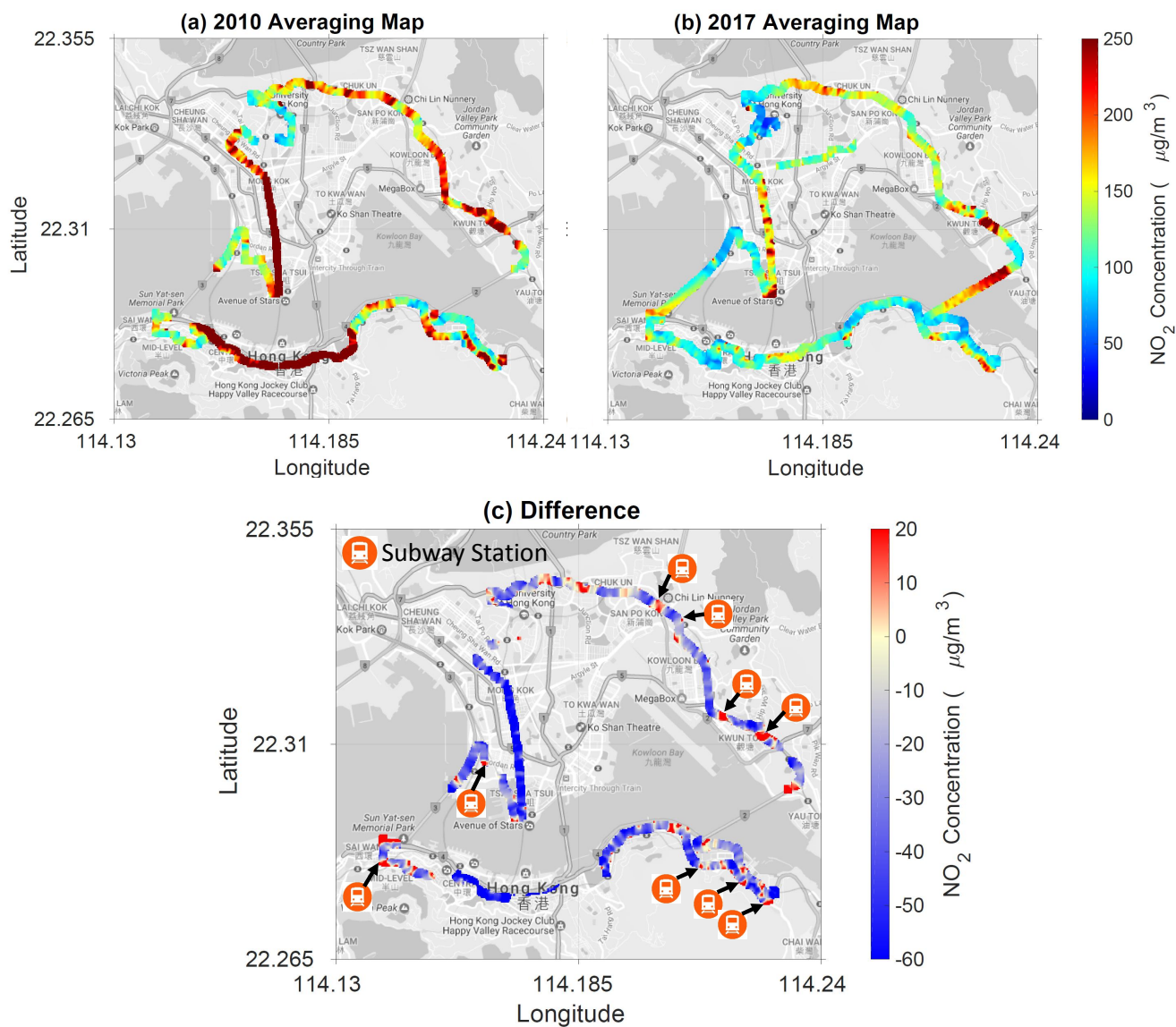
Figure 8. Averaged on-road NO₂ concentrations measured along the standard route during (a) December 2010 and (b) March 2017. (c) shows the relative differences between 2010 and 2017. The markers indicate the location of metro stations. Measurements taken during morning rush hours, noontime and evening rush hours are weighted equally in the averaging.
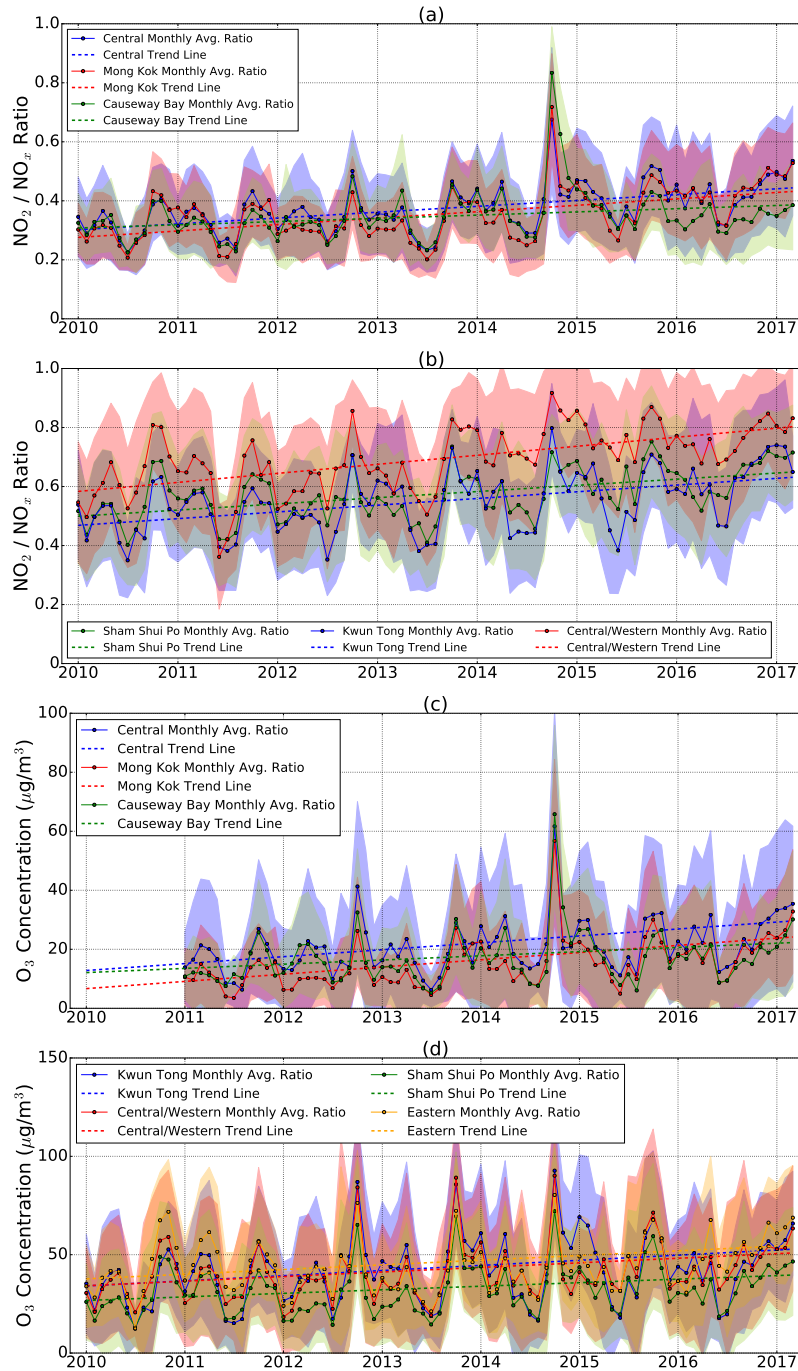
Figure 9. Monthly averaged NO_2/NO_x ratio from EPD (a) roadside stations (b) ambient stations. O_3 concentrations measured by EPD (c) roadside stations (d) ambient stations are shown. Shadowed area indicates the $1\,\sigma$ standard deviation variation of measurements.

system in Hong Kong, the role of bus has gradually changed from point to point long distance services to a connector between destination and metro stations. Therefore, enhancement of NO_2 levels is observed around metro stations. On the other hand, franchised bus operators in Hong Kong started to introduce low emission buses (i.e., Euro IV and V) since 2009. Buses with model earlier than Euro III are proven to be more polluted than latest models (Dallmann et al., 2011; Mock, 2014; Lau et al.,

5 2015; Pastorello and Melios, 2016). Therefore, bus companies started to install retro fit catalytic convertor on earlier bus models and these buses will be replaced completely by buses with higher emission standard by 2021. In addition, the government has set up franchised bus Low Emission Zones (LEZs) in three busiest traffic corridors in Hong Kong on 31st Dec 2015. Buses with emission standard below Euro IV are not allowed to operate within these low emission zones. Therefore, both roadside and its nearby ambient NO_2 levels show a descending trend. Navigation (water transport), road transport and public electricity

10 generation are the largest sources of NO_x according to the 2015 Hong Kong Emission Inventory Report and data from the EPD Hong Kong Air Pollutant Emission Inventory, accounting for 33 %, 30 % and 25 % of total NO_x emissions in 2010 (only NO_x is available in the EPD inventory) and 37 %, 18 % and 28 % in 2016, respectively. NO_x emissions from navigation and public electricity generation are rather constant, while emissions from road transport show a significant reduction of ∼50 % from 32.1 tonnes in 2010 down to 16.2 tonnes in 2015. This is coherent with the decreasing trend of NO_2 from 2010 to 2017.

15 We have looked into the NO_2/NO_x ratio as well as the O_3 concentration in order to better understand the impacts of reduction of vehicular emission of NO_x. An increasing trend of NO_2/NO_x ratio is observed from both roadside and ambient monitoring stations. Figure 9 shows the NO_2/NO_x ratio for (a) roadside and (b) ambient stations. Ozone concentrations from both (c) roadside and (d) ambient stations are shown for reference. Decreasing roadside NO_2 level with increasing NO_2/NO_x ratio implies a significant reduction of primary NO emissions. The reduction of primary NO could be subjected to the upgraded

20 catalytic converter of diesel vehicles (from Euro III or earlier model to Euro IV and V) which reduces the total NO_x emission and increases the NO_2/NO_x ratio (Kašpar et al., 2003). Newer diesel engines in general reduce the total NO_x emission by ∼50 % according to the European emission standards for diesel passenger cars (EU emission standards, 2007). The Euro III diesel engines emission limit of NO_x is 0.50 g/km, whereas the Euro IV emissions limit has been reduced by half to 0.25 g/km. However, this standard might not fully reflect the real driving condition (Franco et al., 2014) and it should be confirmed by more

25 realistic mobile measurements. Furthermore, Tian et al. (2011) observed a rising roadside NO_2/NO_x ratio as well coincided with the introduction of new environmental friendly pre-Euro light and heavy duty vehicles in 2000 and 2003. Ning et al. (2012) also suggested that the proposal of replacing Euro II and III franchised buses to meet Euro IV or even higher emission standards will result in an increase of roadside NO_2/NO_x ratio. In addition, a general rising trend of ambient and roadside ozone is also observed from the EPD monitoring data. The increase of atmospheric NO_2/NO_x with large reduction of NO may

30 be partly related to the recent increase of O_3 level in the ambient, as less NO is available for the titration process under heavy NO_x environment. However, it is difficult to quantify the contribution of increase of ozone on the NO_2/NO_x ratio. Discussion of the interaction between O_3 and NO_x is however beyond of the scope of the paper.
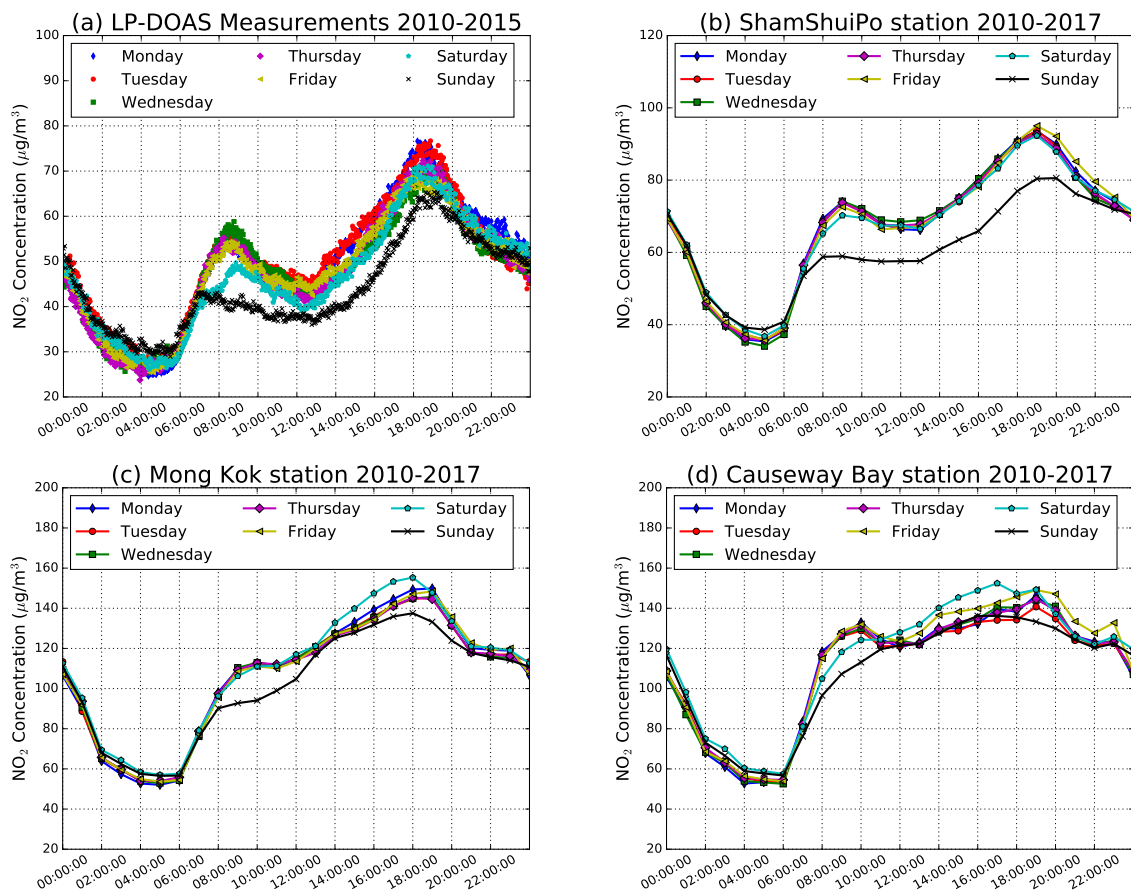
Figure 10. (a) shows the five years average diurnal cycle of NO_2 of each day of the week measured by LP-DOAS.The seven years average diurnal cycle of NO_2 of each day of the week measured by EPD (b) Sham Shui Po station, (c) Mong Kok station and (d) Causeway Bay station.

3.4 Weekend effect

Figure 10a shows the five years average diurnal cycle of NO_2 of each day of the week measured by LP-DOAS, and the seven years average NO_2 diurnal pattern measured by EPD Sham Shui Po, Mong Kok and Causeway Bay station are shown in Figure 10b, c and d, respectively. The diurnal pattern of NO_2 illustrates different characteristics between weekdays and weekend.
5 Different measurement locations also show different characteristics of NO_2 during weekend. The LP-DOAS measurement indicates the NO_2 concentration is on average 3.3 % lower on Saturday and 8.7 % lower on Sunday compared to weekdays. However, the morning rush hour (8:00 to 10:00) peak of NO_2 is significantly reduced by 23.1 % on Sunday, while the evening rush hour (18:00 to 20:00) peak shows a less pronounced reduction of 9.7 %. NO_2 measurements from the Sham Shui Po ambient station and the LP-DOAS show similar diurnal variation pattern and weekend reduction. The weekend reduction is
10 less pronounced for the roadside measurements in Mong Kok, the NO_2 level is on average 3.8 % lower on Sunday compared to weekdays, with reduction during the morning and evening rush hours of 13.1 % and 7.3 %, respectively. Similar weekend reductions are also observed by other EPD roadside stations, i.e., Causeway Bay and Central. These differences in the diurnal cycle are most likely due to different types of land use. Traffic emissions are the main source of NO_2 in urban areas which is strongly dependent on human activities. In residential areas, traffic is reduced during weekend as most of the residents do
15 not work on Sunday, e.g., frequency of buses is reduced during weekend. However, the traffic load is mostly unchanged in commercial areas, since shops are open as well on Sunday.

In order to further investigate the relationship between residents' activities during weekdays and weekend and NO_2 emissions, we have looked into the morning standard route measurements on a sequential Sunday and Monday in 2017. Two sequential days are used for comparison so as to avoid influences from different meteorological conditions. NO_2 concentration
20 maps measured on Sunday and Monday are shown in Figure 11a and b and its difference in c. Coinciding NO_2 concentration measured by the 7 EPD stations are also shown for reference. The NO_2 level on Sunday is on average about 45 % lower than that of Monday. The mobile measurements are in general agreement with coinciding EPD data, while discrepancies can be observed for peak values captured by the more frequently measuring CE-DOAS. This discrepancy is mainly due to the difference in measurement time. Mobile measurement recorded the instant concentration of on-road NO_2 which could
25 easily be influenced by a single incident, especially the on-road NO_2 level varies rapidly. On the other hand, EPD monitors provide hourly averaged NO_2 concentration which tend to average out those local pollution peaks. Besides, four EPD ambient monitoring stations are located more than 15 m above ground level. Therefore, EPD ambient stations are expected to measure lower NO_2 concentrations compared to on-road CE-DOAS measurements. In addition, NO_2 concentrations of each location show rapid changes which are highly dependent on the traffic flow. However, a consistent elevated NO_2 level is ob-
30 served over the most busy roads, such as Nathan Road in Kowloon, western and eastern Harbor Cross Harbor tunnels. 85 % of the measurements show significant higher (>1 ppbv) NO_2 concentrations, whereas 13 % of the measurements show significant lower (>1 ppbv) NO_2 concentrations on Monday compared to Sunday. The spatial pattern of elevated NO_2 level on Sunday matches with the location of large shopping malls. Similar difference maps between other workdays and Sunday are observed. The number of licensed private car grows by $\sim$30 % from 415 thousands in 2010 to 536 thousands in 2016, while
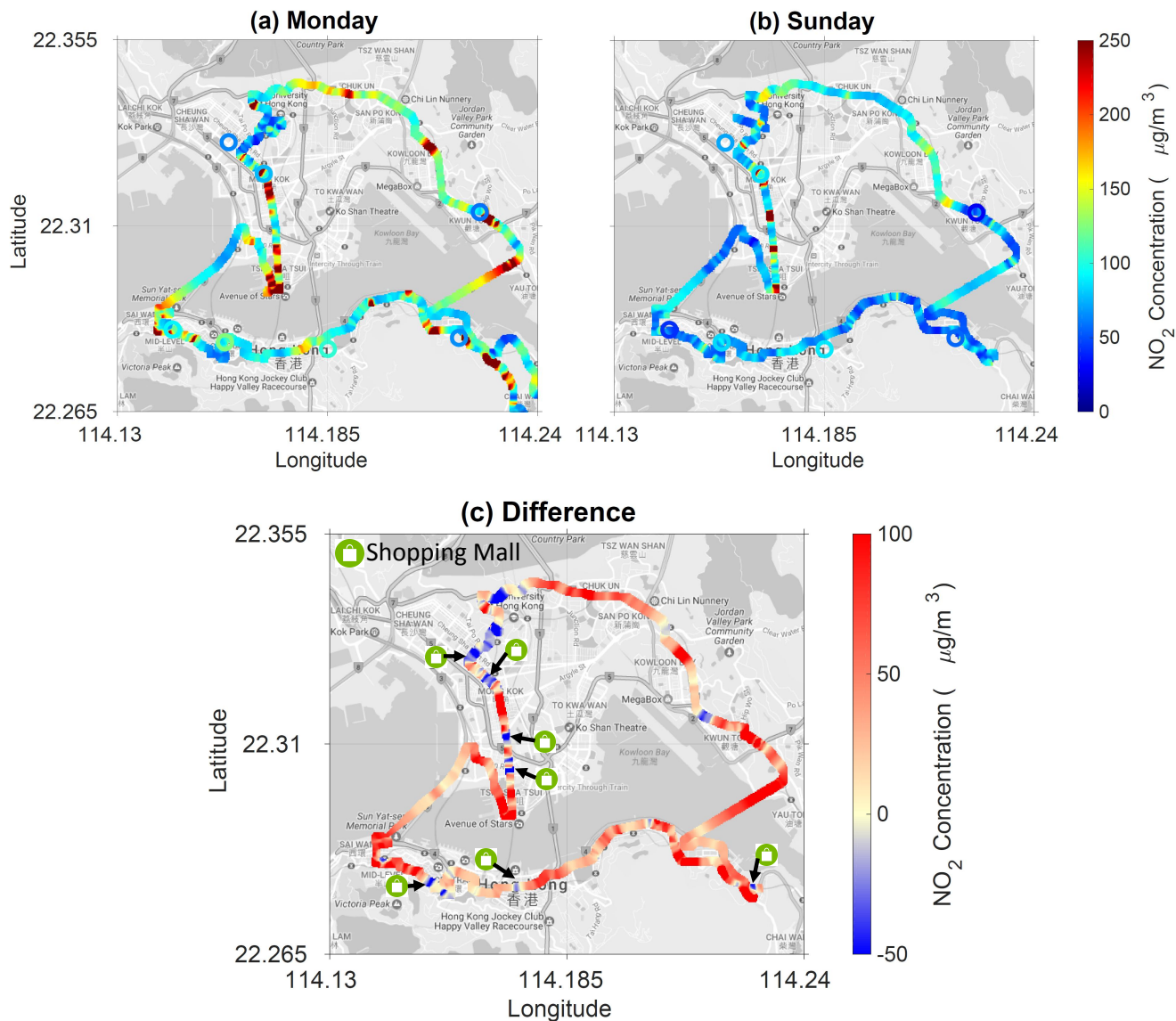
Figure 11. Mobile CE-DOAS measurement of on-road NO_2 on (a) Monday (6th Mar 2017) and (b) Sunday (5th Mar 2017). Coinciding NO_2 concentration measured by the 7 EPD stations are shown on the map as circle markers for reference. The color scale of the EPD measurements is the same as the mobile measurements. (c) shows the differences between Monday and Sunday. The markers indicate the location of major shopping malls.

the public transport usage increases by $\sim 9\,\%$ from 11.6 millions time per day in 2010 to 12.6 millions time per days in 2016 (http://www.td.gov.hk/en/transport_in_hong_kong/transport_figures/monthly_traffic_and_transport_digest/index.html). These numbers implied that the usage per private car is greatly reduced. The decrease of private car usage is mainly due to the reduction for daily commute using private cars, which is coherent with the increase of public transport usage. As a result most of the private cars are mainly used during weekends in Hong Kong. People are taking public transport for daily commute to avoid traffic jam during weekdays, while go shopping with their own car in the weekend. As the parking spaces are limited around these shopping areas and results in low speed cruising and traffic congestion around these major shopping areas during weekend. As a consequence, an enhancement of NO_2 level can be observed over these locations. This is an interesting example of how people's daily life influences the pollution patterns.

3.5   Spatial distribution of NO_2 in Hong Kong

In order to have a better overview of major pollution hotspots in Hong Kong, all measurements taken in 2010 were spatially averaged to a high resolution grid of $20\,\mathrm{m} \times 20\,\mathrm{m}$ (Figure 12 (a)). These measurements covered most of the major roads in Hong Kong, including highway, urban, sub-urban and rural area. As the spatial coverage of measurements taken in 2010 and 2017 is quite different and there is a general decreasing trend of NO_2, we only use data measured in 2010 for the spatial distribution analysis to avoid any bias toward lower value over the city center. Elevated NO_2 levels are mainly distributed over motorways and busy roads that always with high traffic intensity in the city center, e.g. No. 8 and No. 9 motorway, Nathan Road in Kowloon, Queen's Road in Central, and Hennessy Road from Admiralty to Causeway Bay. About 29 % of the on-road measurements exceeded the WHO one hour guideline value of $200\,\mu\mathrm{g/m^3}$, while 27 % of the data measured in the city center exceed the guideline. High NO_2 values over motorways are probably due to having more heavy-duty vehicles. On the other hand, traffic congestion and street canyon effects (Rakowska et al., 2014) are the major cause of elevated on-road NO_2 in the city center.

As described in section 3.2.2, on-road pollutants mainly produced by vehicles and the traffic flow patterns also have a large impact on pollutant distributions (Westerdahl et al., 2005; Kaur et al., 2007; Huan and Kebin, 2012; Rakowska et al., 2014; Fu et al., 2017). The diurnal dependency of the measurement times is corrected for using the simultaneous normalized LP-DOAS measurement. The normalized spatial distribution of on-road NO_2 is shown in Figure 12(b). This normalized dataset provides a better overview of the daily average. NO_2 levels over some regions are significantly enhanced after applying the normalization, particularly, the residential area in Yuen Long district and Tung Chung district, where the Hong Kong International airport is located. Some other areas (mainly at the city center and highways) obtained lower NO_2 values after normalization. Enhancement of NO_2 concentrations after normalization for certain areas is due to the fact that the mobile measurement took place during non-peak hours during the day, while reduction of NO_2 concentrations is due to the measurement vehicle overpassing the regions during rush hours of the day. Compared to unnormalized data, only 27 % of normalized on-road measurements exceeded the WHO one hour guideline and about 20 % of the area in the city center exceed the guideline. The slightly decreased NO_2 level in both all over Hong Kong and city center are presumably due to the fact that the measurement campaigns are conducted during daytime when the NO_2 level is in general higher compared to nighttime.
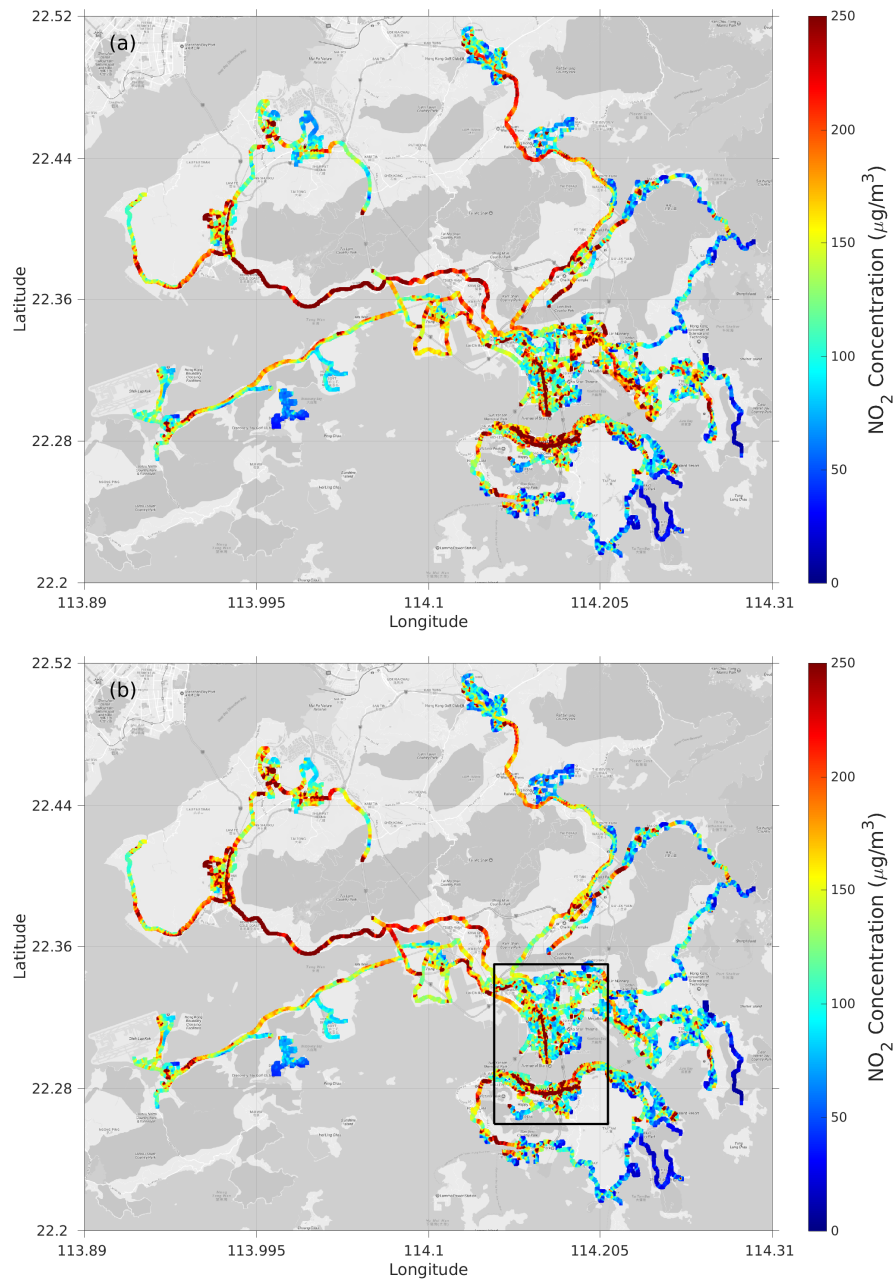
Figure 12. (a) Averaged spatial distribution of NO₂ in Hong Kong measured by the mobile CE-DOAS in 2010. (b) Normalized spatial distribution of NO₂ over Hong Kong measured by the mobile CE-DOAS in 2010. The CE-DOAS data is normalized using coinciding normalized LP-DOAS data. The black box indicates the area of the city center used for the other maps. The standard route measurement was performed 3 times per day, while other locations only have single or few overpasses during the two campaigns.

4 Summary and conclusions

A high resolution spatial distribution map of street level NO_2 makes identifing city pollution hotspots possible. It could meanwhile provide valuable information for urban planning as well as help with the development of pollution control measures. For obtaining the pollutant information, on-road mobile CE-DOAS measurements were successfully deployed in Hong Kong in December 2010 and March 2017, respectively. The diurnal dependency due to the different sampling time of mobile measurements was normalized through combining the continuous measurements of LP-DOAS. Furthermore, the algorithm, which was developed to separate and filter the accumulation of local emissions due to traffic congestion, helped us focusing on the concentrations instead of the stopping frequency while the maps' comparison.

The long term trend and spatial variations of ambient, roadside and on-road NO_2 levels were investigated by analyzing on-road CE-DOAS measurements together with LP-DOAS and EPD monitor stations. The long term trend analysis showed that the ambient NO_2 level was descending with a rate of 2.5 % per year, while the roadside NO_2 level showed a strong decreasing trend with annual reduction rate ranging from 3.4 - 4.9 %. This observation matched with the mobile measurement results that on-road NO_2 was in general reduced by 20 - 50 % between 2010 and 2017. The changes of the operational strategies of the major franchised bus company in Hong Kong could be revealed by the enhancements of NO_2 level observed at locations close to metro stations. In addition, a rising trend of NO_2/NO_x ratio was observed in both roadside and ambient monitor data. This was mainly subjected to the reduction of vehicle emissions which typically associated with NO_2/NO_x ratio. Increasing O_3 concentration also contributed to the reduction of NO_2 level in the past few years in Hong Kong.

The temporal emission characteristic of different districts in Hong Kong were investigated using mobile measurements taken on different days of the week. The weekend reduction rate of on-road measurements was much higher than the long term ambient / roadside observation of LP-DOAS and EPD monitoring stations. By analyzing the spatial pattern of the weekend reduction effect, we found that the NO_2 levels of most residential districts were reduced on Sunday while commercial and shopping areas showed a rather constant NO_2 level throughout the week. The mobile CE-DOAS measurements presented in this paper offered a full-scaled perception for the on-road NO_2 characteristics in Hong Kong. Simultaneously, these spatial distribution measurement results are also important for chemical transport model validations and assessment of human health effects.

Data availability. The mobile measurement data is available on request from the corresponding author (ka.chan@dlr.de).

Competing interests. The authors declare that they have no conflict of interest.

Acknowledgements. The work described in this paper was jountly supported by the German Academic Exchange Service (DAAD) Programme des Projektbezogenen Personenaustauschs (PPP) (project ID: 57334317), the Germany / Hong Kong Joint Research Scheme spon-

sored by the Research Grants Council of Hong Kong and the German Academic Exchange Service (Reference No. G-CityU104/16) and the Research Grants Council of the Hong Kong Special Administrative Region, China (Project No. CityU 11305817). We thank Annette Schütt, Teng Fei, Song Hao, Willy Ying for helping with the organization of the measurement campaign.

References

Bond, D. W., Zhang, R., Tie, X., Brasseur, G., Huffines, G., Orville, R. E., and Boccippio, D. J.: NO_x production by lightning over the continental United States, Journal of Geophysical Research: Atmospheres, 106, 27 701–27 710, https://doi.org/10.1029/2000JD000191, http://dx.doi.org/10.1029/2000JD000191, 2001.

5   Bucsela, E. J., Krotkov, N. A., Celarier, E. A., Lamsal, L. N., Swartz, W. H., Bhartia, P. K., Boersma, K. F., Veefkind, J. P., Gleason, J. F., and Pickering, K. E.: A new stratospheric and tropospheric NO_2 retrieval algorithm for nadir-viewing satellite instruments: applications to OMI, Atmospheric Measurement Techniques, 6, 2607–2626, https://doi.org/10.5194/amt-6-2607-2013, 2013.

Carslaw, D. C.: Evidence of an increasing NO_2/NO_x emissions ratio from road traffic emissions, Atmospheric Environment, 39, 4793–4802, https://doi.org/10.1016/j.atmosenv.2005.06.023, http://www.sciencedirect.com/science/article/pii/S1352231005005443, 2005.

10   Chan, K., Wiegner, M., Wenig, M., and Pöhler, D.: Observations of tropospheric aerosols and NO_2 in Hong Kong over 5 years using ground based MAX-DOAS, Science of The Total Environment, https://doi.org/https://doi.org/10.1016/j.scitotenv.2017.10.153, 2017a.

Chan, K. L., Pöhler, D., Kuhlmann, G., Hartl, A., Platt, U., and Wenig, M. O.: NO_2 measurements in Hong Kong using LED based long path differential optical absorption spectroscopy, Atmospheric Measurement Techniques, 5, 901–912, https://doi.org/10.5194/amt-5-901-2012, https://www.atmos-meas-tech.net/5/901/2012/, 2012.

15   Chan, K. L., Wang, S., Liu, C., Zhou, B., Wenig, M. O., and Saiz-Lopez, A.: On the summertime air quality and related photochemical processes in the megacity Shanghai, China, Science of The Total Environment, 580, 974–983, https://doi.org/http://dx.doi.org/10.1016/j.scitotenv.2016.12.052, 2017b.

Chang, Y., Zou, Z., Deng, C., Huang, K., Collett, J. L., Lin, J., and Zhuang, G.: The importance of vehicle emissions as a source of atmospheric ammonia in the megacity of Shanghai, Atmospheric Chemistry and Physics, 16, 3577–3594, https://doi.org/10.5194/acp-16-3577-2016, https://www.atmos-chem-phys.net/16/3577/2016/, 2016.

20   Dallmann, T. R., Harley, R. A., and Kirchstetter, T. W.: Effects of diesel particle filter retrofits and accelerated fleet turnover on drayage truck emissions at the Port of Oakland, Environmental science & technology, 45, 10 773–10 779, https://doi.org/10.1021/es202609q, 2011.

EU emission standards: European Union emission standards for new light duty vehicles (passenger cars and light commercial vehicles), https://www.dieselnet.com/standards/eu/ld.php#stds, directive 98/69/EC, DieselNet. Accessed: 2018-02-06, 2007.

25   Fiedler, S. E., Hese, A., and Ruth, A. A.: Incoherent broad-band cavity-enhanced absorption spectroscopy, Chemical Physics Letters, 371, 284–294, https://doi.org/http://dx.doi.org/10.1016/S0009-2614(03)00263-X, 2003.

Franco, V., Sánchez, F. P., German, J., and Mock, P.: Real-world exhaust emissions from modern diesel cars, communications, 49, 847 129–102, 2014.

Fu, X., Liu, J., Ban-Weiss, G. A., Zhang, J., Huang, X., Ouyang, B., Popoola, O., and Tao, S.: Effects of canyon geometry on the 30   distribution of traffic-related air pollution in a large urban area: Implications of a multi-canyon air pollution dispersion model, Atmospheric Environment, 165, 111–121, https://doi.org/10.1016/j.atmosenv.2017.06.031, http://www.sciencedirect.com/science/article/pii/S1352231017304120, 2017.

Hermans, C., Vandaele, A. C., Carleer, M., Fally, S., Colin, R., Jenouvrier, A., Coquart, B., and Mérienne, M.-F.: Absorption cross-sections of atmospheric constituents: NO_2, O_2, and H_2O, Environmental Science and Pollution Research, 6, 151–158, 35   https://doi.org/10.1007/BF02987620, https://doi.org/10.1007/BF02987620, 1999.

Huan, L. and Kebin, H.: Traffic Optimization: A New Way for Air Pollution Control in China's Urban Areas, Environmental Science & Technology, 46, 5660–5661, https://doi.org/10.1021/es301778b, https://doi.org/10.1021/es301778b, pMID: 22612715, 2012.

Huang, R.-J., Zhang, Y., Bozzetti, C., Ho, K.-F., Cao, J.-J., Han, Y., Daellenbach, K. R., Slowik, J. G., Platt, S. M., Canonaco, F., et al.: High secondary aerosol contribution to particulate pollution during haze events in China, Nature, 514, 218–222, 2014.

Jang, M. and Kamens, R. M.: Characterization of Secondary Aerosol from the Photooxidation of Toluene in the Presence of NO_x and 1-Propene, Environmental Science & Technology, 35, 3626–3639, https://doi.org/10.1021/es010676+, 2001.

5 Kašpar, J., Fornasiero, P., and Hickey, N.: Automotive catalytic converters: current status and some perspectives, Catalysis Today, 77, 419–449, https://doi.org/10.1016/S0920-5861(02)00384-X, http://www.sciencedirect.com/science/article/pii/S092058610200384X, fundamentals of Catalysis and Applications to Environmental Problems, 2003.

Kaur, S., Nieuwenhuijsen, M., and Colvile, R.: Fine particulate matter and carbon monoxide exposure concentrations in urban street transport microenvironments, Atmospheric Environment, 41, 4781–4810, https://doi.org/10.1016/j.atmosenv.2007.02.002, http://www.
10 sciencedirect.com/science/article/pii/S1352231007001343, 2007.

Keuken, M., Roemer, M., and van den Elshout, S.: Trend analysis of urban NO_2 concentrations and the importance of direct NO_2 emissions versus ozone/NOx equilibrium, Atmospheric Environment, 43, 4780–4783, https://doi.org/10.1016/j.atmosenv.2008.07.043, http://www. sciencedirect.com/science/article/pii/S1352231008006298, urban Air Quality, 2009.

Kraus, S.: DOASIS A Framework Design for DOAS, Ph.D. thesis, Combined Faculties for Mathematics and for Computer Science, Univer-
15 sity of Mannheim, 2005.

Krotkov, N. A., Lamsal, L. N., Celarier, E. A., Swartz, W. H., Marchenko, S. V., Bucsela, E. J., Chan, K. L., Wenig, M., and Zara, M.: The version 3 OMI NO_2 standard product, Atmospheric Measurement Techniques, 10, 3133–3149, https://doi.org/10.5194/amt-10-3133-2017, 2017.

Kuhlmann, G., Lam, Y. F., Cheung, H. M., Hartl, A., Fung, J. C. H., Chan, P. W., and Wenig, M. O.: Development of a custom OMI
20 NO_2 data product for evaluating biases in a regional chemistry transport model, Atmospheric Chemistry and Physics, 15, 5627–5644, https://doi.org/10.5194/acp-15-5627-2015, 2015.

Langridge, J. M., Ball, S. M., and Jones, R. L.: A compact broadband cavity enhanced absorption spectrometer for detection of atmospheric NO_2 using light emitting diodes, Analyst, 131, 916–922, 2006.

Lau, C. F., Rakowska, A., Townsend, T., Brimblecombe, P., Chan, T. L., Yam, Y. S., Močnik, G., and Ning, Z.: Evaluation of diesel
25 fleet emissions and control policies from plume chasing measurements of on-road vehicles, Atmospheric Environment, 122, 171–182, https://doi.org/10.1016/j.atmosenv.2015.09.048, http://www.sciencedirect.com/science/article/pii/S1352231015303903, 2015.

Levelt, P., Van den Oord, G. H. J., Dobber, M., Malkki, A., Visser, H., de Vries, J., Stammes, P., Lundell, J., and Saari, H.: The ozone monitoring instrument, Geoscience and Remote Sensing, IEEE Transactions on, 44, 1093–1101, https://doi.org/10.1109/TGRS.2006.872333, 2006.

30 Longley, I., Somervell, E., and Gray, S.: Roadside increments in PM_{10}, NOx and NO_2 concentrations observed over 2 months at a major highway in New Zealand, Air Quality, Atmosphere & Health, 8, 591–602, https://doi.org/10.1007/s11869-014-0305-4, https://doi.org/10. 1007/s11869-014-0305-4, 2015.

Marchenko, S., Krotkov, N. A., Lamsal, L. N., Celarier, E. A., Swartz, W. H., and Bucsela, E. J.: Revising the slant column density retrieval of nitrogen dioxide observed by the Ozone Monitoring Instrument, Journal of Geophysical Research: Atmospheres, 120, 5670–5692,
35 https://doi.org/10.1002/2014JD022913, http://dx.doi.org/10.1002/2014JD022913, 2014JD022913, 2015.

Min, K.-E., Washenfelder, R. A., Dubé, W. P., Langford, A. O., Edwards, P. M., Zarzana, K. J., Stutz, J., Lu, K., Rohrer, F., Zhang, Y., and Brown, S. S.: A broadband cavity enhanced absorption spectrometer for aircraft measurements of glyoxal, methylglyoxal, nitrous

acid, nitrogen dioxide, and water vapor, Atmospheric Measurement Techniques, 9, 423–440, https://doi.org/10.5194/amt-9-423-2016, https://www.atmos-meas-tech.net/9/423/2016/, 2016.

Mock, P.: European vehicle market statistics, Pocketbook: Lugano, Switzerland, 2014.

Muilwijk, C., Schrijvers, P., Wuerz, S., and Kenjereš, S.: Simulations of photochemical smog formation in complex urban areas, Atmospheric Environment, 147, 470–484, https://doi.org/10.1016/j.atmosenv.2016.10.022, http://www.sciencedirect.com/science/article/pii/S1352231016308299, 2016.

Ning, Z., Wubulihairen, M., and Yang, F.: PM, NO_x and butane emissions from on-road vehicle fleets in Hong Kong and their implications on emission control policy, Atmospheric Environment, 61, 265–274, https://doi.org/10.1016/j.atmosenv.2012.07.047, http://www.sciencedirect.com/science/article/pii/S1352231012007194, 2012.

Pastorello, C. and Melios, G.: Explaining road transport emissions: a non-technical guide, Tech. rep., European Environment Agency, 2016.

Platt, U., Meinen, J., Pöhler, D., and Leisner, T.: Broadband Cavity Enhanced Differential Optical Absorption Spectroscopy (CE-DOAS) – applicability and corrections, Atmospheric Measurement Techniques, 2, 713–723, https://doi.org/10.5194/amt-2-713-2009, https://www.atmos-meas-tech.net/2/713/2009/, 2009.

Rakowska, A., Wong, K. C., Townsend, T., Chan, K. L., Westerdahl, D., Ng, S., Močnik, G., Drinovec, L., and Ning, Z.: Impact of traffic volume and composition on the air quality and pedestrian exposure in urban street canyon, Atmospheric Environment, 98, 260–270, https://doi.org/10.1016/j.atmosenv.2014.08.073, http://www.sciencedirect.com/science/article/pii/S1352231014006840, 2014.

Rothman, L., Barbe, A., Benner, D. C., Brown, L., Camy-Peyret, C., Carleer, M., Chance, K., Clerbaux, C., Dana, V., Devi, V., Fayt, A., Flaud, J.-M., Gamache, R., Goldman, A., Jacquemart, D., Jucks, K., Lafferty, W., Mandin, J.-Y., Massie, S., Nemtchinov, V., Newnham, D., Perrin, A., Rinsland, C., Schroeder, J., Smith, K., Smith, M., Tang, K., Toth, R., Auwera, J. V., Varanasi, P., and Yoshino, K.: The HITRAN molecular spectroscopic database: edition of 2000 including updates through 2001, Journal of Quantitative Spectroscopy and Radiative Transfer, 82, 5–44, https://doi.org/10.1016/S0022-4073(03)00146-8, http://www.sciencedirect.com/science/article/pii/S0022407303001468, the HITRAN Molecular Spectroscopic Database: Edition of 2000 Including Updates of 2001., 2003.

Rotman, D. A., Tannahill, J. R., Kinnison, D. E., Connell, P. S., Bergmann, D., Proctor, D., Rodriguez, J. M., Lin, S. J., Rood, R. B., Prather, M. J., Rasch, P. J., Considine, D. B., Ramaroson, R., and Kawa, S. R.: Global Modeling Initiative assessment model: Model description, integration, and testing of the transport shell, Journal of Geophysical Research: Atmospheres, 106, 1669–1691, https://doi.org/10.1029/2000JD900463, 2001.

Solomon, S., Schmeltekopf, A. L., and Sanders, R. W.: On the interpretation of zenith sky absorption measurements, Journal of Geophysical Research: Atmospheres, 92, 8311–8319, https://doi.org/10.1029/JD092iD07p08311, 1987.

Thalman, R. and Volkamer, R.: Inherent calibration of a blue LED-CE-DOAS instrument to measure iodine oxide, glyoxal, methyl glyoxal, nitrogen dioxide, water vapour and aerosol extinction in open cavity mode, Atmospheric Measurement Techniques, 3, 1797–1814, https://doi.org/10.5194/amt-3-1797-2010, https://www.atmos-meas-tech.net/3/1797/2010/, 2010.

Tian, L., Hossain, S. R., Lin, H., Ho, K. F., Lee, S. C., and Yu, I. T. S.: Increasing trend of primary NO_2 exhaust emission fraction in Hong Kong, Environmental Geochemistry and Health, 33, 623–630, https://doi.org/10.1007/s10653-011-9375-5, https://doi.org/10.1007/s10653-011-9375-5, 2011.

Uhrner, U., von Löwis, S., Vehkamäki, H., Wehner, B., Bräsel, S., Hermann, M., Stratmann, F., Kulmala, M., and Wiedensohler, A.: Dilution and aerosol dynamics within a diesel car exhaust plume-CFD simulations of on-road measurement conditions, Atmospheric Environment, 41, 7440–7461, https://doi.org/10.1016/j.atmosenv.2007.05.057, http://www.sciencedirect.com/science/article/pii/S1352231007005006, 2007.

Vandaele, A. C., Hermans, C., Fally, S., Carleer, M., Colin, R., Mérienne, M.-F., Jenouvrier, A., and Coquart, B.: High-resolution Fourier transform measurement of the NO_2 visible and near-infrared absorption cross sections: Temperature and pressure effects, Journal of Geophysical Research: Atmospheres, 107, ACH 3–1–ACH 3–12, https://doi.org/10.1029/2001JD000971, http://dx.doi.org/10.1029/2001JD000971, 4348, 2002.

5   Venables, D. S., Gherman, T., Orphal, J., Wenger, J. C., and Ruth, A. A.: High sensitivity in situ monitoring of NO_3 in an atmospheric simulation chamber using incoherent broadband cavity-enhanced absorption spectroscopy, Environmental science & technology, 40, 6758–6763, 2006.

Vogt, R., Scheer, V., Casati, R., and Benter, T.: On-Road Measurement of Particle Emission in the Exhaust Plume of a Diesel Passenger Car, Environmental Science & Technology, 37, 4070–4076, https://doi.org/10.1021/es0300315, https://doi.org/10.1021/es0300315, pMID:

10   14524437, 2003.

Volkamer, R., Spietz, P., Burrows, J., and Platt, U.: High-resolution absorption cross-section of glyoxal in the UV–VIS and IR spectral ranges, Journal of Photochemistry and Photobiology A: Chemistry, 172, 35–46, https://doi.org/10.1016/j.jphotochem.2004.11.011, http://www.sciencedirect.com/science/article/pii/S1010603004005143, 2005.

Washenfelder, R., Langford, A., Fuchs, H., and Brown, S.: Measurement of glyoxal using an incoherent broadband cavity enhanced absorp-

15   tion spectrometer, Atmospheric Chemistry and Physics, 8, 7779–7793, 2008.

Westerdahl, D., Fruin, S., Sax, T., Fine, P. M., and Sioutas, C.: Mobile platform measurements of ultrafine particles and associated pollutant concentrations on freeways and residential streets in Los Angeles, Atmospheric Environment, 39, 3597–3610, https://doi.org/10.1016/j.atmosenv.2005.02.034, http://www.sciencedirect.com/science/article/pii/S1352231005002232, 2005.

Zhang, R., Tie, X., and Bond, D. W.: Impacts of anthropogenic and natural NO_x sources over the U.S. on tropospheric chemistry, Proceedings

20   of the National Academy of Sciences, 100, 1505–1509, https://doi.org/10.1073/pnas.252763799, 2003.